Time-dependent coherent light pulse absorption from macroscopic Maxwell equations

Marie-Laure Chavazas [1] and Quentin Remy [2,1,*]
[1] *Université de Lorraine, CNRS, IJL, F-54000 Nancy, France*
[2] *Cavendish Laboratory, University of Cambridge, Cambridge, United Kingdom*

(Received 17 June 2022; revised 12 July 2022; accepted 12 July 2022; published 21 July 2022)

We present a simple way to calculate the time-dependent energy transfer between a general pulse of light and a layered media. Although we argue that trying to define such absorption is, in general, meaningless, our model still improves the standard method by including effects such as chromatic dispersion, more accurate time dependence of absorption, and nonabsorptive effects.

DOI: 10.1103/PhysRevB.106.014310

I. INTRODUCTION

With the advent of subpicosecond laser pulses, it has been required to model the transient out-of-equilibrium response of condensed matter systems to an ultrashort stimulus. Some examples include the study of the disparate dynamics for electrons and phonons in metals [1], nonthermal electronic dynamics in metals [2] and semiconductors [3], ultrafast magnetization dynamics of metals [4], dielectrics [5], semiconductors [6], and half-metals [7], the melting of the superconducting phase [8], nonlinear optics for instance for THz generation via optical rectification [9], or the heating and machining of polymers [10]. Even though a dynamical treatment of the interaction between a coherent light pulse and matter is possible using quantum methods such as the real-time time dependent density functional theory [11] (rt-TDDFT) or density matrix approaches [12], it is still often more practical to use a semiclassical treatment where the light pulse is seen as a transient external source of energy, for instance, in a two-temperature model [13] (2TM) or in a Boltzmann transport calculation [14]. In such case, one often resorts to the transfer matrix method (TMM) in various frameworks [15–21] to compute light propagation and the subsequent light absorption as a function of depth in the considered system. In this case, the energy transfer from the external electromagnetic radiation to the condensed matter system is inferred from Poynting theorem:

$$\frac{\partial u}{\partial t} + \nabla \cdot \boldsymbol{S} = -\boldsymbol{J} \cdot \boldsymbol{E}. \tag{1}$$

We shall refer to this equation as the microscopic Poynting theorem in contrast to the macroscopic version given below. The electromagnetic energy density u is given by $u = (\varepsilon_0 \boldsymbol{E}^2 + \boldsymbol{B}^2/\mu_0)/2$ with ε_0 and μ_0 the vacuum permittivity and permeability, respectively, while $\boldsymbol{E}$ and $\boldsymbol{B}$ are the electric field and magnetic induction respectively. $\boldsymbol{S} = (\boldsymbol{E} \times \boldsymbol{B})/\mu_0$ is the Poynting vector,[1] while $\boldsymbol{J}$ is the charge current. Equation (1) means that energy transported by the electromagnetic field (left-hand side) may be transferred (lost by the electromagnetic field) to matter (right-hand side). The right-hand side of this equation can then be used to calculate light absorption provided that one has an equation for $\boldsymbol{J}$. In TMM calculations, it is usually assumed that the external light source is a monochromatic wave and one averages the physical quantities of interest over a period of oscillation of the electromagnetic field. The absorption (energy gained by matter) is either obtained from $-\nabla \cdot \boldsymbol{S}$ or $\boldsymbol{J} \cdot \boldsymbol{E}$. Both methods can be found in the literature (see, for instance, Ref. [17] or [22]). The assumption that the electromagnetic radiation is monochromatic implies that it is fundamentally of infinite extension in time. The time dependence of the absorption of a pulse is then often modeled by taking the absorption amplitude proportional to the measured intensity profile of the light pulse. The TMM calculation itself only serves to obtain the spatial dependence of the absorption.

One directly sees that this approach is not rigorously correct to predict light absorption of pulses since they have a certain spectral range. This will lead to a more complicated time dependence of the absorption (influenced by interferences between different monochromatic waves and reflections within the layered material system) as well as chromatic dispersion due to the frequency dependence of refractive indices. Our extension of the TMM to include such effects is presented in Sec. II. We then present some example calculations of this model in Sec. III. We find that chromatic dispersion, which cannot be modeled in the standard TMM, leads to quantitative changes of the (time averaged) absorption profile. They may become significant for laser pulses with a duration of a few femtoseconds or less provided that one knows refractive indices for a sufficiently large range of frequencies. Additional predictions of this model will lead us to discuss the validity and meaning of the underlying assumptions of our model in Sec. IV. In particular, we give an extensive discussion of conservation of energy in the context of macroscopic Maxwell

*Corresponding author: quentinremy5@gmail.com

[1] The general validity of the expression of Poynting vector as shown here has been discussed before and is beyond the scope of this work. Because we consider nonmagnetic materials with no spatial dispersion, the expression $\boldsymbol{S} = \boldsymbol{E} \times \boldsymbol{H}$ should still be valid [41–43].

 ©2022 American Physical Society

equations and conclude that the problem of energy transfer is in general ill-defined in this framework, unveiling a paradigm similar to the Abraham-Minkowski controversy for electromagnetic energy.

II. MODEL

We now present our model for the energy transfer from a coherent pulse of electromagnetic radiation to matter. The material systems considered are usually thin films, or the electromagnetic radiation has normal incidence, such that we only consider spatial dependence along the direction z orthogonal to the sample surface. The presented model can be easily extended to the general three dimensional case. We first start by a description of coherent light pulses before considering their propagation in heterostructures via the TMM and finally their absorption.

A. Coherent pulses

We first only discuss electromagnetic fields in vacuum which are described by Maxwell equations without sources. As mentioned above, considering a monochromatic wave implies having an infinite pulse duration. In order to model a pulse with a finite duration, one needs to consider a superposition of monochromatic waves. We only consider plane waves, assuming that the electric field in an actual electromagnetic field beam is orthogonal to its wave vector. This is usually a good approximation for optical laser pulses and typical experimental setups [23]. The external complex (with a tilde) electromagnetic radiation incident on the material as a function of time t and space z is then given by

$$\widetilde{\boldsymbol{E}}(z,t) = E_0\hat{\boldsymbol{e}}\sum_n G(\omega_n)e^{i(k_n z-\omega_n t)}, \tag{2a}$$

$$\widetilde{\boldsymbol{B}}(z,t) = E_0\sum_n \frac{(\boldsymbol{k}_n\times\hat{\boldsymbol{e}})}{\omega_n}G(\omega_n)e^{i(k_n z-\omega_n t)}. \tag{2b}$$

E_0 is the amplitude of the electric field whose polarization axis is defined by the unit vector $\hat{\boldsymbol{e}}$ (we will only consider s and p linear polarizations). Because we only consider plane waves, the wave vectors $\boldsymbol{k}_n$ all have the same directions specified by an angle of incidence θ_0 (see Appendix B). Only their norm $k_n = \|\boldsymbol{k}_n\| = \omega_n/c$ (in vacuum) is different for different monochromatic waves indexed by the subscript n. In Eq. (2), we only consider an electromagnetic field propagating in one direction. In our one-dimensional model, the total electromagnetic field is the superposition of forward and backward propagating fields (see Appendix B). G is a complex spectral density which governs the shape of the light pulse. It should be remembered that the quantities representing the true electromagnetic field are real quantities (without a tilde). This is especially important in this work as we do not consider quantities averaged over a period of oscillation. One must then take the real part of Eq. (2) when calculating quantities such as energy or Poynting vector but the complex version of each field is still convenient for calculations noting that the real part operator is linear. The angular frequencies $\omega_n = n\pi c/L$ are integer multiples of the fundamental angular frequency of a fictitious Fabry-Pérot interferometer with a length L. This means that Eq. (2) describes in general a periodic repetition of pulses separated in space by a length $2L$. When $L\to\infty$, the sum in Eq. (2) becomes an integral and represents the Fourier transform of the spectral density. The parameter L can be adjusted so as to reproduce the repetition rate of a laser. For simulations, L is high enough so as to model the effect of only a single pulse.

B. Approximations and transfer matrix method

We now consider electromagnetic fields in matter as well as in vacuum, which are described by macroscopic Maxwell equations [24]. A full knowledge of the macroscopic fields is then obtained provided that one has an equation for charge and current distributions. Electromagnetic waves propagation is fully characterized by refractive indices in the absence of external sources of charges and/or currents [25]. These indices are fully described by the behavior of free charges (via Ohm's Law) and bound states (via the permittivity and permeability tensors in the usual dipolar approximation [24]). It is also assumed that the permeability tensor is equal to the unit tensor (assumption valid for optical frequencies and for non magnetic materials at THz frequencies) so that $\boldsymbol{B} = \mu_0\boldsymbol{H}$. We further neglect any possible anisotropy (such as birefringence or gyrotropy), nonlinear effects, spatial dispersion, and time inhomogeneity. Thus our materials are described by a frequency-dependent scalar refractive index [26], which is the most commonly available data in the literature [27]. Finally, we only consider s and p polarized light (otherwise one needs the four by four TMM formalism [21]). Thus, for each monochromatic wave in the electromagnetic pulse, the electromagnetic field propagation can be computed from the standard TMM. Then, because we only consider linear media, the propagation of the electromagnetic pulse Eq. (2) within any heterostructure is computed by summing the electric and magnetic fields (in matter we more conveniently consider magnetic field instead of magnetic induction) associated with each monochromatic mode. In each layer of the heterostructure, each monochromatic wave of the electromagnetic field is characterized by the amplitude of the forward and backward propagating modes as well as the angle of incidence (complex in general) of the wave vector. We refer to standard literature about the TMM formalism for details [15–21]. Here, we compute the monochromatic waves propagation using the implementation of Byrnes [20]. The complete electromagnetic field as a function of time and space for s and p polarizations is given in Appendix B. In particular, what we need from the standard TMM formalism are the electric field amplitudes E_{0n}^f and E_{0n}^b of forward and backward modes of monochromatic waves n, as well as the complex angles θ_n.

C. Absorption for pulses

We can know tackle the problem of energy absorption. We first start by highlighting the main difference between our approach and the conventional one to calculate the latter quantity. In the standard TMM, the starting point is the time

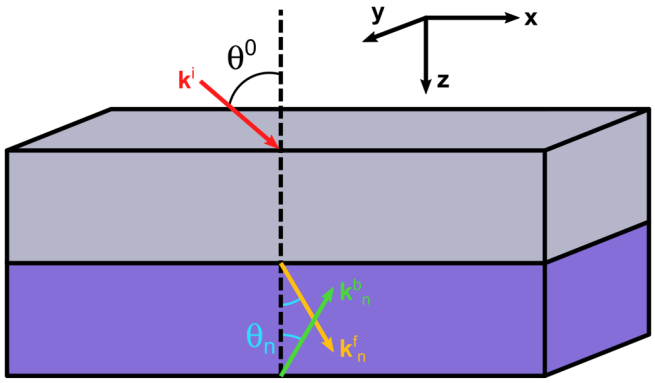

FIG. 1. Geometrical configuration of wave vectors for light absorption calculations in multilayers. We represented the wave vector of the incident electromagnetic field as well as the wave vectors for forward and backward propagations in one of the layers and for one wavelength.

averaged Poynting vector $\mathrm{Re}(\widetilde{\boldsymbol{E}} \times \widetilde{\boldsymbol{H}}^{\star})/2$.[2] Here, we calculate the complete Poynting vector $\boldsymbol{S} = \boldsymbol{E} \times \boldsymbol{H} = \mathrm{Re}(\widetilde{\boldsymbol{E}}) \times \mathrm{Re}(\widetilde{\boldsymbol{H}})$. However, as in the standard TMM, we calculate the absorption from $-\nabla \cdot \boldsymbol{S}$ and not $\boldsymbol{J} \cdot \boldsymbol{E}$. This is because the latter form requires a knowledge of $\boldsymbol{J}$, usually via Ohm's law, on top frequency-dependent conductivities, and it does not consider absorption due to bound states. The former on the other hand only depends on knowing complex refractive indices [26]. This is extensively discussed in Sec. IV. Because we are only interested in the energy absorption integrated over the x and y coordinates (see Fig. 1) and because there is no electromagnetic field in a region infinitely far from the irradiated area of the material system, the energy absorption as a function of time and depth is defined as $A(z,t) \equiv -\partial S_z/\partial z$, where S_z is the z component of the Poynting vector. We first focus on the normalized absorption $a(z,t) = A(z,t)/S_z^0$ with $S_z^0 = S_z(z=0, t=0)$. We then find

$$\begin{aligned}
\text{(s)}: \quad a(z,t) &= \frac{-1}{S_z^0} \sum_{n,m} \mathrm{Re}\left[ik_n\left(E_n^f - E_n^b\right)\right] \\
&\quad \times \mathrm{Re}\left[\frac{\widetilde{n}_m}{c\mu_0}\left(E_m^f - E_m^b\right)\cos(\theta_m)\right] \\
&\quad + \sum_{n,m} \mathrm{Re}\left[E_n^f + E_n^b\right] \\
&\quad \times \mathrm{Re}\left[\frac{\widetilde{n}_m}{c\mu_0} ik_m\left(E_m^f + E_m^b\right)\cos(\theta_m)\right], \quad \text{(3a)} \\
\text{(p)}: \quad a(z,t) &= \frac{-1}{S_z^0} \sum_{n,m} \mathrm{Re}\left[ik_n\left(E_n^f + E_n^b\right)\cos(\theta_n)\right] \\
&\quad \times \mathrm{Re}\left[\frac{\widetilde{n}_m}{c\mu_0}\left(E_m^f + E_m^b\right)\right] \\
&\quad + \sum_{n,m} \mathrm{Re}\left[\left(E_n^f - E_n^b\right)\cos(\theta_n)\right] \\
&\quad \times \mathrm{Re}\left[\frac{\widetilde{n}_m}{c\mu_0} ik_m\left(E_m^f - E_m^b\right)\right], \quad \text{(3b)}
\end{aligned}$$

$$S_z^0 = \sum_{n,m} \frac{E_0^2}{c\mu_0} G(\omega_n) G(\omega_m) \cos(\theta^0). \quad \text{(3c)}$$

With $\widetilde{n}_m$ the refractive index for the monochromatic mode m, θ_0 the angle of incidence of the incident (external) light pulse, and $E_n^f(z,t)$ and $E_n^b(z,t)$ are given in Appendix B. This definition is discussed in details in the remaining part of this work. Equation (3) shows that one does not need to know E_0 to calculate the normalized absorption. For applications however, it is often required to know the absorption. It is then desired to explicitly compute S_z^0. If, as often, one only knows the fluence F of a light pulse, one must use the fact that the integral of the Poynting vector over time, in the direction of propagation of the pulse, is equal to the light fluence. This is presented in Appendix A for the case of a Gaussian pulse. To compare with the standard result of the TMM, we need to define a time independent normalized absorption $a(z)$. It is obtained by the requirement that the energy density $u(z)$ provided locally by the light pulse to the heterostructure is $u(z) = a(z)F$. This means that $a(z)$ is obtained by

$$a(z) = \frac{1}{F} \int A(z,t)dt. \quad (4)$$

Where the integral must be performed over a time interval that contains only a single pulse from the periodic repetition of Eq. (2). If chromatic dispersion is negligible, the latter equation will provide a result that is close to the standard TMM procedure.[3] From the time independent absorption calculated with the standard TMM, the time-dependent absorption is usually phenomenologically obtained as the time dependence of the light intensity profile. However, the true time dependence will be in general completely different, even without chromatic dispersion, due to interferences between monochromatic waves and reflections inside the heterostructures which can lead, for instance, to echoes. Finally, we note that not only absorption but also time-dependent transmission and reflection of a coherent light pulse may be calculated by calculating the Poynting vector in vacuum on both sides of the heterostructure, for backward and forward pulses, respectively.

III. RESULTS

We now present some example calculations of this model for a simple Pt(5 nm)/Cu(10 nm) heterostructure on a transparent substrate. We only present simulations at normal incidence and so light polarization becomes unimportant. We first consider a Gaussian optical pulse and simulate the pulse

[2]Within the same approximation, absorption can also be calculated equivalently from reflection and transmission [17] because the formula for the latter two quantities are obtained from the time averaged Poynting vector for the backward wave in the initial medium (reflection) and the forward wave in the final medium (transmission).

[3]This is not generally the case because Eq. (4) depends on frequency via refractive indices as well as wave vectors $\|k_n\| = \omega_n \widetilde{n}_n/c$.

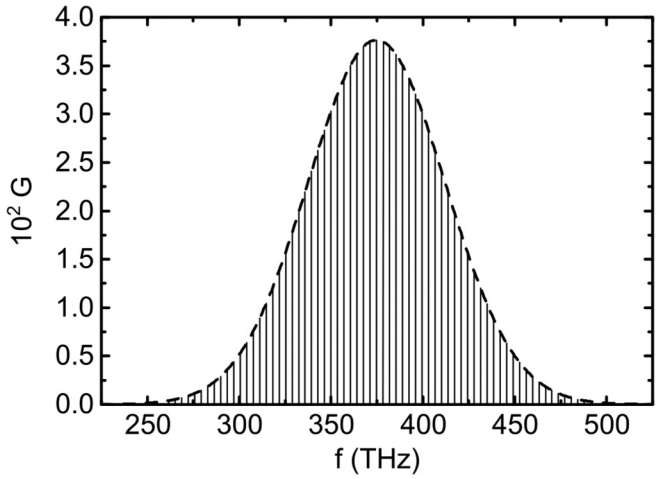

FIG. 2. Spectral density G of the optical pulse used for simulations as a function of frequency $f = \omega/(2\pi)$. The dashed line represents the function given by Eq. (A1) while vertical lines represent the selected frequencies for simulations.

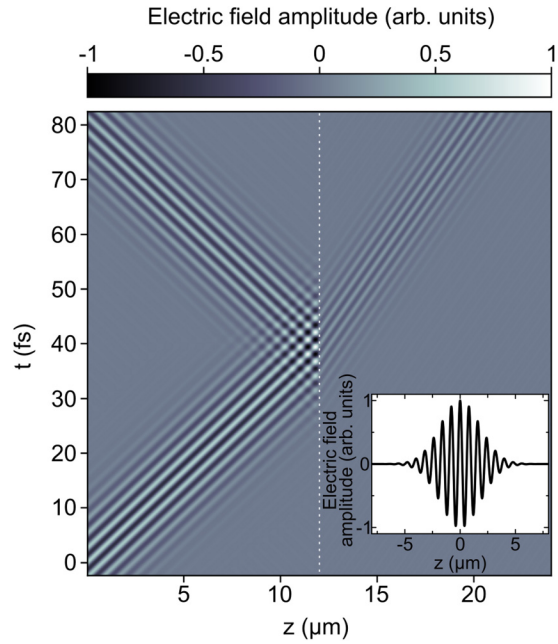

FIG. 3. Electric field amplitude as a function of time t and position z. The air/Pt interface of the sample is at a position $z = 12$ μm (white dashed line). The inset show the electric field amplitude for $t = 0$ fs.

propagation and absorption. We also use the calculated absorption as an input for the early stage of a two temperature model (2TM) calculation. We finish by comparing the results obtained at THz frequencies.

A. Optical pulses

We first consider an optical light pulse of central angular frequency $\omega_c = 2\pi c/\lambda_0$, with $\lambda_0 = 800$ nm the wavelength in vacuum, and pulse duration $\tau = 10$ fs (see Appendix A). For such pulse durations, the spatial extension of the pulse along the direction of propagation is of the order of 10 μm which is much smaller than typical substrate thicknesses. We thus consider that the substrate is infinite and choose a glass substrate. The system of interest is then air/Pt(5 nm)/Cu(10 nm)/glass where both air ($\widetilde{n} = 1$) and glass media are considered as semi infinite.

The spectral density of the pulse is shown in Fig. 2. Because our electromagnetic field corresponds to a periodic repetition of pulses [Eq. (2)], the spectral density is discrete and the relevant information is represented as the vertical lines. The separation in frequency between each line is given by the length L previously introduced and we use here $L = 10\sqrt{2}\tau c$ ($\sqrt{2}\tau$ is the duration of the electromagnetic amplitude pulse $\propto \|\boldsymbol{E}\|$, while τ is the duration of the electromagnetic intensity pulse $\propto \|\boldsymbol{E}\|^2$). The amplitude of each selected mode is then given by Eq. (A1) and shown as a dashed line in Fig. 2. Note that for this optical pulse, we chose a real spectral density. The refractive index for air and glass are 1 and 1.5136 for the considered frequency range and the refractive index for Cu ($\widetilde{n} = 0.11 + 5.14i$ at ω_c) and Pt ($\widetilde{n} = 2.98 + 6.37i$ at ω_c) are taken from the literature [28,29].

1. Propagation

By computing the electric field as a superposition of all monochromatic waves in each medium [Eq. (2a) in air; see Appendix B in general] based on the assumption of linear media, one can predict how an electromagnetic pulse behaves as it encounters the Pt/Cu/glass sample. This is shown in Fig. 3 where we plotted the electric field amplitude $\|\boldsymbol{E}(z,t)\|$. The electric field amplitude at $t = 0$ fs is shown in the inset and has the usual shape of a Gaussian pulse as expected. For longer times, one can see the pulse being partially reflected by the metallic sample and also partially transmitted. The amplitude of the transmitted field is visibly lower because of the thickness of the considered metallic heterostructure and one can clearly see that the light velocity and wavelength are smaller due to the fact that the semi-infinite medium on the right-hand side is glass. The checkerboard pattern around $t = 40$ fs on the left-hand side of the sample clearly shows interferences between the incident and reflected pulses. One can also observe the π phase shift occurring when light is reflected from a medium with a higher refractive index. Such calculations can in general reproduce pulse damping and dispersion [23] like the Telegrapher's equation does, as it should, since both our approach and the Telegrapher's equation are based on Maxwell equations.

2. Absorption, the role of dispersion and comparison with the monochromatic case

Next we compute the light absorption in the sample according to Eq. (3). In Fig. 4, we show the time dependence of light absorption for given positions. In Fig. 4(a), we show absorption in Pt at the air/Pt interface. A first important difference compared to the usually modeled time-dependent absorption is the presence of oscillations due to the coherent nature of the calculation. Also, we see that absorption can sometimes be negative, i.e., the electromagnetic field retrieves some of the energy it provided to matter. We shall come back to this point in the next section. We already note however that the

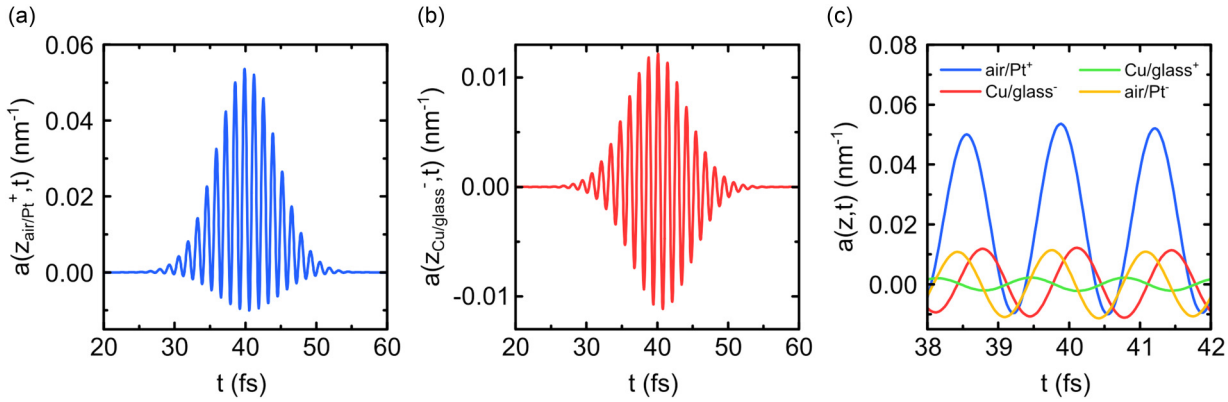

FIG. 4. Calculated time-dependent light absorption in (a) Pt at the air/Pt interface and in (b) Cu at the Cu/glass interface. (c) shows a zoom around 40 fs for positions around air/Pt and Cu/glass interfaces. Plus and minus superscripts indicate whether the position of interest is the right side (+) or the left side (−) of an interface.

plotted function is on average (in time) positive. In Fig. 4(b), we show absorption in Cu at the Cu/glass interface. In this case, absorption is also positive in average as we shall see below, even though this is less obvious. The reason is that at these frequencies Cu absorbs much less than Pt.

The time dependence of the absorption within each layer is almost independent of position because layers are really thin (only the amplitude changes as shown in Fig. 5). In general, because of the finite velocity of light, there might be a non negligible phase shift between the time-dependent absorption at different position within a layer, but this requires layers at least a few hundreds of nanometers thick. There is however a significant phase shift at interfaces. This is clearly shown in Fig. 4(c) where we consider absorption on both sides of the air/Pt and Cu/glass interfaces. The reason for this phase shift is the fact that the (frequency-dependent) transmission and reflection coefficients obtained from Fresnel equations are in general complex since refractive indices themselves are complex numbers. We note that absorption in air and glass is not identically zero for reasons we will explain in the next section, but it is exactly zero when integrated over time.

We now compare our results with the standard TMM by computing the time independent absorption according to Eq. (4). The results are shown in Fig. 5. Figure 5(a) shows almost no difference between our method and the standard TMM. This is because refractive indices actually do not change much with frequencies for the considered spectral density (Fig. 2). We recover the fact that absorption, when integrated over time, must be positive (and is exactly zero in media with a real refractive index; not shown). There is, however, a drastic change in the optical properties of Cu for photon energies of around 2.1 eV (590 nm wavelength; 508 THz frequency), which is barely covered by the spectrum of Fig. 2, due to interband transitions [30]. Hence, we also calculated the time integrated absorption for a central wavelength of 600 nm in Fig. 4(b). For the same pulse duration of 10 fs, we see an increased difference with the monochromatic case. This difference is further increased if we use a pulse duration of 4 fs. We however could not decrease the pulse duration even more because of the lack of data for sufficiently high and low frequencies. Interestingly, a significant difference in absorption is also observed in Pt while dispersion ($d\tilde{n}/d\omega$) is

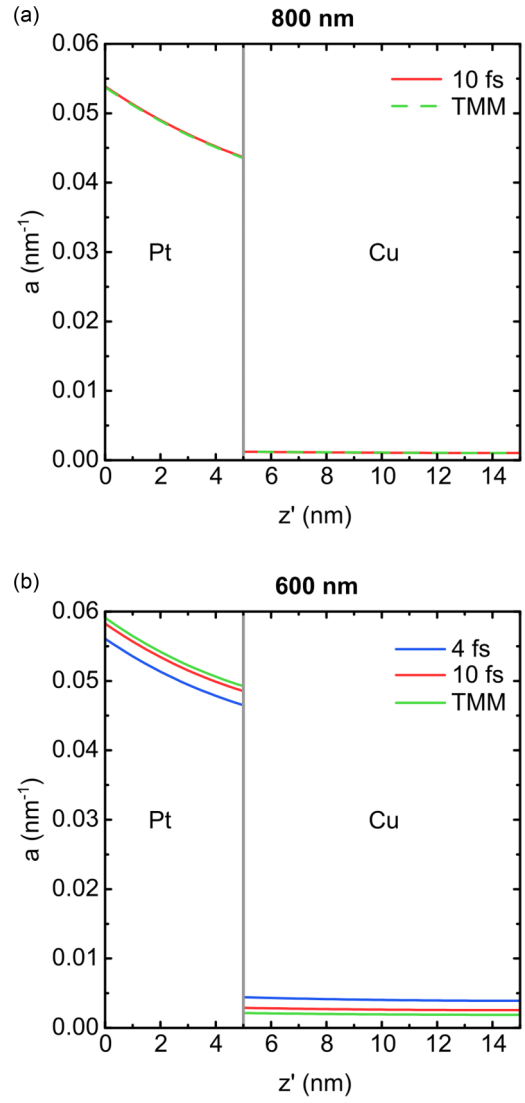

FIG. 5. Time integrated absorption as a function of depth $z' = z - 12\,\mu$m in the sample computed for a central wavelength of (a) 800 and (b) 600 nm and for various pulse durations. Results obtained with the standard TMM method (monochromatic/infinite pulse duration) are also shown.

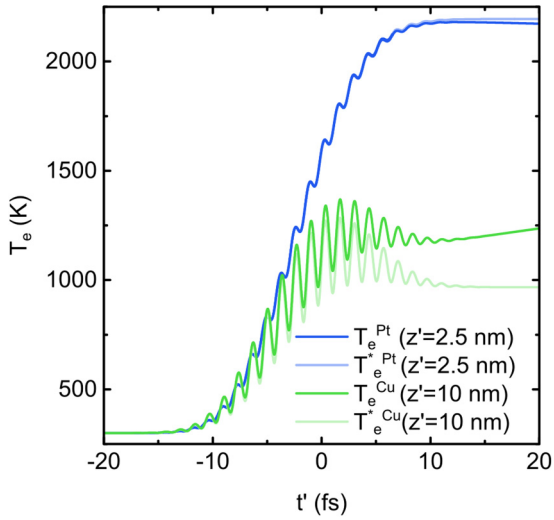

FIG. 6. Calculated electronic temperature in the metallic structure as obtained by the 2TM and the calculated time-dependent absorption. We give the electronic temperature for two depths $z' = 2.5$ nm (Pt) and $z' = 10$ nm (Cu). Temperatures $T^\star$ are obtained by neglecting electronic diffusion and the electron-phonon interaction in the 2TM. The time axis has been shifted by defining $t' = t - 40$ fs. The (measured [23]) fluence used for simulations is 1.84 mJ/cm^2. The relatively high electronic temperature in Cu considering its low absorption is due to its relatively low heat capacity, around an order of magnitude lower than for Pt.

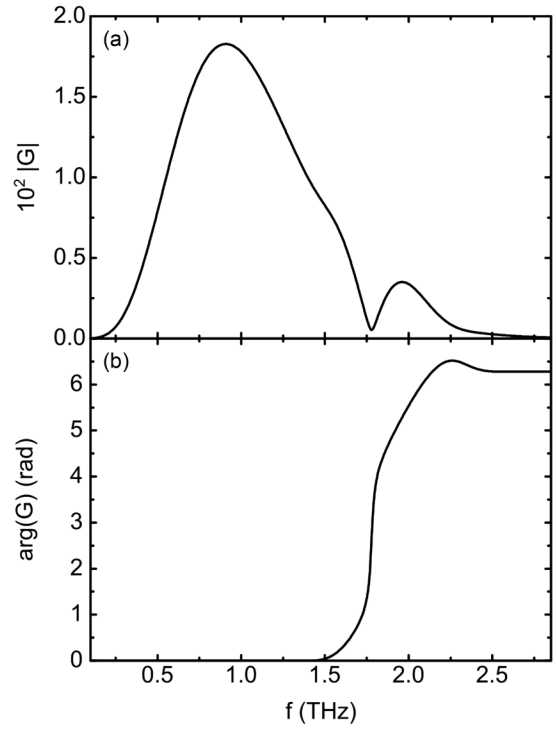

FIG. 7. Spectral density G of the optical pulse used for simulations as a function of frequency $f = \omega/(2\pi)$. The top panel (a) shows the norm of the spectral density while the bottom panel (b) shows its argument. Contrary to Fig. 2, we do not show explicitly the discrete nature of the spectral density because frequency difference between each mode is too small to be displayed.

almost identical for both 600 and 800 nm. Finally, we note that significant differences of absorption profiles may also be obtained for longer pulse durations (around 100 fs) in more complex multilayer structures [23].

3. Consequence on condensed matter dynamics

Our model may have direct consequences for models of condensed matter systems that do not rigorously simulate the light matter interaction. To illustrate this, we consider the simple case of the 2TM with methods and parameters as detailed in Refs. [23,31]. The main point is to use $A(z,t) = a(z,t)S_z^0$ as the energy source term in the 2TM. The results are shown in Fig. 6.

We only focus on the electronic temperature T_e at instants when the light pulse is still interacting with the metallic structure. As expected from Fig. 4, the electronic temperature increases in a non monotonous way, coherently with the light pulse. Of course the validity of the 2TM (and the existence of such fast oscillations in the electronic temperature) is especially dubious at this timescale but it allows us to simply illustrate the transfer of energy between light and matter happening within the framework of macroscopic Maxwell equations we introduced earlier. To make this even simpler, we also made calculations neglecting the electron-phonon interaction (negligible at this timescale) and electronic transport (here diffusion). We call the resulting temperature $T_e^\star$ and plot it in Fig. 6 for the same depths as earlier. The role of electronic diffusion is then evidenced and one can clearly see the heat transport from the highly excited Pt layer towards the Cu layer. Our main focus is however the shape of $T_e^\star$: the superposition of a pulsed oscillation with a sigmoid. A similar behavior is also obtained from rt-TDDFT [32] for the charge motion. It is understood from the existence of absorptive and nonabsorptive processes during light matter interaction [33] which is inherently present in the formalism we use via the real and imaginary parts of the refractive index.

Another consequence of our model on light matter interaction simulations is due to the observed phase shift in Fig. 4(c). This phase shift means that the electric field and/or the absorption may have different signs in different layers. Considering that charge transport happens at the sub-femtosecond timescale [34], this effect may have an important effect in condensed matter systems excited by ultrashort light pulses. The authors are not aware of any work in this direction.

B. THz pulses

We finish this section by showing similar calculations but for THz pulses which have become a widely used tool to excite and probe condensed matter [35–37]. The spectral density we now consider is shown in Fig. 7.

We consider a more complicated spectral density whose analytical expression is given in Appendix C. The substrate is replaced by a Si substrate. Considering that the light pulse now has a size of a few millimeters, we consider a finite substrate with a thickness of 0.25 mm. For simulations, we now use $L = 20\sqrt{2}\tau c$. The refractive indices were obtained from [38,39] with $\tilde{n} = n + in$ and $n = \sqrt{\sigma_{\mathrm{DC}}/(2\varepsilon_0\omega)}$ where

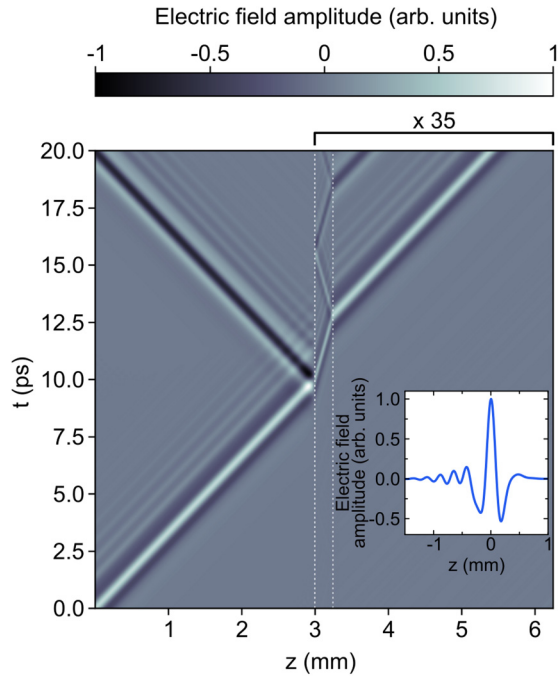

FIG. 8. Electric field amplitude for the THz pulse as a function of time t and position z. The air/Pt interface of the sample is at a position $z = 3$ mm (left white dashed line) while the Si/air interface is at a position $z = 3{,}25$ mm (right white dashed line). The amplitude of the electric field after the air/Pt interface has been multiplied by a factor of 35. The inset show the electric field amplitude for $t = 0$ fs.

σ_{DC} is the DC conductivity [40]. At 1 THz, $n \simeq 509$ for Cu and $n \simeq 186$ for Pt. Similarly to the optical case, we plot the propagation of the THz pulse, as it encounters the multilayer structure, in Fig. 8.

Because of the large reflection, we increased the electric field amplitude after that interface by a factor of 35. This makes the various reflections inside the Si substrate clearly visible. Because of the larger wavelengths considered in this example we find, as expected, that the electric field inside the metallic multilayer is a constant function of space to a good approximation (i.e., the electric field amplitude is almost the same in Pt and in Cu at all instants). In addition, even though refractive indices strongly depend on frequency, no effect of dispersion is expected (because the propagation factors $\exp(ikz)$ are almost equal to 1), which is indeed what we observe. From these results, the absorption in the Pt/Cu structure is calculated as before and shown in Fig. 9.

As for the optical case, the absorption as we calculate it is not zero for a given instant in air and Si, even though its value is smaller than in the metallic layers. The time integrated absorption is however zero, as it should. Again, the time dependence of the absorption is an oscillating function, as calculated before, for instance, in Ref. [22]. However, the absorption is in this case mostly positive (the calculated minimum value is around $-2 \times 10^{-6}\,\mathrm{nm}^{-1}$) which is explained by the higher sample reflectivity at THz frequencies (see Sec. IV). Because the electric field is constant throughout the metallic multilayer, absorption is almost independent of space in a given layer.

Finally, we use the calculated absorption as an input for a 2TM calculation and show the electronic temperature for two positions in the metallic multilayer in Fig. 10. In this case, the electric field amplitude and fluence are related to each other by numerically integrating the computed Poynting

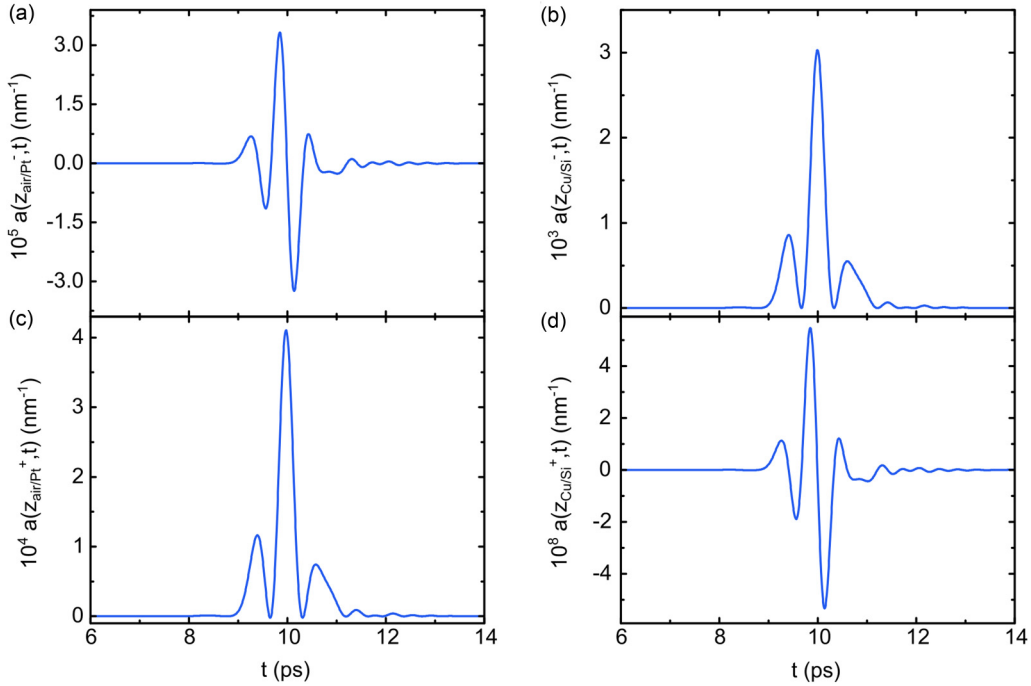

FIG. 9. Calculated time-dependent light absorption in (a) air at the air/Pt interface, in (b) Cu at the Cu/Si interface, in (c) Pt at the air/Pt interface and in (d) in Si at the Cu/Si interface. Plus and minus superscripts indicate whether the position of interest is the right side (+) or the left side (−) of an interface.

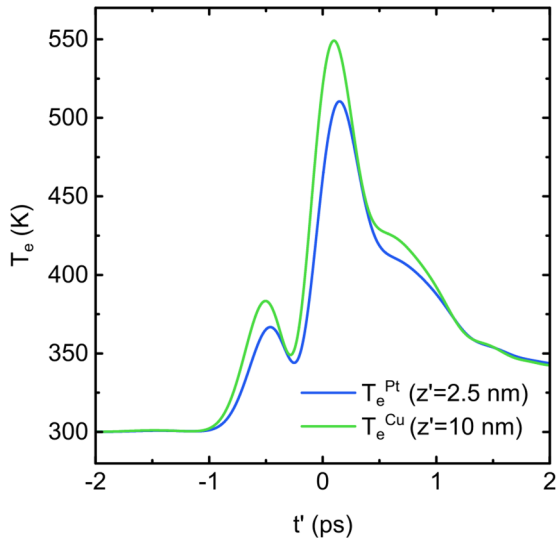

FIG. 10. Calculated electronic temperature in the metallic structure as obtained by the 2TM and the calculated time-dependent absorption for the THz pulse. We give the electronic temperature for two depths $z' = 2.5$ nm (Pt) and $z' = 10$ nm (Cu). The time axis has been shifted by defining $t' = t - 10$ ps and the depth axis by defining $z' = z - 3$ mm. The fluence used for simulations is 0.92 mJ/cm^2.

vector for the incident pulse. One can see that the evolution of the electronic temperature is mostly dominated by the three peaks of absorption observed in Figs. 9(b) and 9(c). Even though absorption is strongly different between Pt and Cu, the calculated electronic temperature is almost the same at both positions for all times. This is due to the fast electronic transport (diffusion in this model) compared to the THz pulse duration.

IV. DISCUSSION

A. The energy conservation equation

The definitions of absorption given earlier ($-\nabla \cdot \boldsymbol{S}$ or $\boldsymbol{J} \cdot \boldsymbol{E}$) are ambiguous. To have a better understanding of this, one needs to look at conservation of energy in detail. Certain approaches to derive the equation for conservation of energy tend to suggest that one can unambiguously separate the energy due to the electromagnetic field from the energy of matter [41]. In such case, absorption is uniquely given by $\boldsymbol{J} \cdot \boldsymbol{E}$. A better description of light-matter interaction can be obtained from the lagrangian of quantum electrodynamics.[4] Field theory straightforwardly gives an equation for the conservation of energy [44]:

$$\frac{\partial e}{\partial t} + \nabla \cdot \boldsymbol{T} = 0, \tag{5a}$$

$$e = u + \psi^\dagger \left(c\boldsymbol{\alpha} \cdot (\boldsymbol{p} - q\boldsymbol{A}) + mc^2\beta\right)\psi, \tag{5b}$$

$$\boldsymbol{T} = \boldsymbol{S} + \frac{c^2}{2}(\psi^\dagger \boldsymbol{p}\psi - (\boldsymbol{p}\psi^\dagger)\psi), - c^2\psi^\dagger q\boldsymbol{A}\psi + \nabla \times \left(\psi^\dagger \frac{\hbar c^2}{4}\bar{\boldsymbol{\sigma}}\psi\right), \tag{5c}$$

where ψ is the electron bispinor field, $\boldsymbol{\alpha}$ and β are the matrices appearing in Dirac equation, $\boldsymbol{p} = -i\hbar\nabla$, $q = -|e|$ is the electron charge, $\boldsymbol{A}$ is the vector potential, m is the electron mass and $\bar{\boldsymbol{\sigma}} = \boldsymbol{\sigma} \otimes \boldsymbol{I}_2$ with $\boldsymbol{\sigma}$ the vector of Pauli matrices and $\boldsymbol{I}_2$ the two by two unity matrix. As shown by Eq. (5) the quantity that is time invariant and that can thus be safely defined as energy is the volume integral of the total energy density e. Attempting to define the energy of light and matter as two separate quantities, such as, for instance, u and $\psi^\dagger(c\boldsymbol{\alpha} \cdot \boldsymbol{p} + mc^2\beta)\psi$, respectively, would be devoted of sense in general because of the term $cq\psi^\dagger\boldsymbol{\alpha} \cdot \boldsymbol{A}\psi$. This term depends of both matter and electromagnetic fields and could thus be assigned to either the energy of light or matter or even shared between light and matter. Only when both fields are sufficiently well separated in space, such that $\psi^\dagger\boldsymbol{\alpha} \cdot \boldsymbol{A}\psi \simeq 0$ everywhere in space, one can unambiguously define the energy of light and matter [44]. The same is obviously true for the energy current $\boldsymbol{T}$ and momentum density $\boldsymbol{T}/c^2$. This inevitably leads to the impossibility of defining without ambiguity quantities such as light absorption (this work) or the momentum of light (the Abraham-Minkowski controversy, see, for instance, Ref. [46]) in a general manner. Any separation is fundamentally based on an approximation (which may depend on the chosen gauge). A similar conclusion can be drawn for any interacting system, such as a mixture of electrons and phonons in the framework of the 2TM used in the previous section, where energies of each subsystem are defined as the energies (often renormalized [47]) of the noninteracting parts of an Hamiltonian.

B. Macroscopic Maxwell equations and the definition of light absorption

Properly calculating energy transfers therefore requires to completely account for interactions which is usually an impossible task in practice. The question our work tries to answer, which is "What is the amount of energy acquired by matter, from light, at each moment in time?" does not have a proper answer. Nonetheless, it is still helpful to provide a qualitative answer to this question in many semiclassical problems. We thus come back to the framework of macroscopic Maxwell equations. In this case, the equation that is used to describe transfers of energy, the macroscopic Poynting theorem, is [24]

$$\boldsymbol{E} \cdot \frac{\partial \boldsymbol{D}}{\partial t} + \boldsymbol{H} \cdot \frac{\partial \boldsymbol{B}}{\partial t} + \nabla \cdot (\boldsymbol{E} \times \boldsymbol{H}) = -\boldsymbol{J} \cdot \boldsymbol{E}. \tag{6}$$

Even in this framework, one deals with ambiguities to define the energy of the electromagnetic field because of the light-matter interaction. First, it is well-known that in general no electromagnetic energy density can be defined even mathematically, because the first two terms of the left-hand side of Eq. (6) cannot be written as the time derivative of any quantity [24,48]. Even in simpler cases, where such quantity can

[4]We only need to consider a classical electron field. One can consider several fields for matter (such as a field for nuclei) but this is unimportant for our discussion. No quantum field theory is required for our explanation of conservation laws. Such theory is required to understand renormalization effects necessary to properly consider self interactions. This is however beyond the scope of this work and we do not discuss self-fields [45].

be defined mathematically, ambiguities still remain. We first consider the standard case of a light pulse which is sufficiently long such that chromatic dispersion are small in the range of frequencies where the spectral density is considerable and the spectral density is mostly centered around a central angular frequency ω_c [24]. Then Eq. (6) becomes

$$\begin{aligned}\frac{\partial u_{\text{eff}}}{\partial t}+\nabla\cdot\boldsymbol{S} &= -\boldsymbol{J}\cdot\boldsymbol{E}-\omega_c\,\mathrm{Im}(\varepsilon(\omega_c))\,\langle E^2\rangle \\ &\quad -\omega_c\,\mathrm{Im}(\mu(\omega_c))\,\langle H^2\rangle\,, \qquad (7a)\\ u_{\text{eff}} &= \frac{1}{2}\,\mathrm{Re}\left(\frac{d(\omega\varepsilon)}{\mathrm{d}\omega}(\omega_c)\right)\langle E^2\rangle \\ &\quad +\frac{1}{2}\,\mathrm{Re}\left(\frac{d(\omega\mu)}{\mathrm{d}\omega}(\omega_c)\right)\langle H^2\rangle\,. \qquad (7b)\end{aligned}$$

Angular brackets denote a time average over a period $2\pi/\omega_c$. From this equation, it is clear that both definitions $-\nabla\cdot\boldsymbol{S}$ and $\boldsymbol{J}\cdot\boldsymbol{E}$ contain different contributions to energy transfers, even if the effective electromagnetic energy density u_{eff} could be defined as the true electromagnetic energy density. The definition $\boldsymbol{J}\cdot\boldsymbol{E}$ has the advantage of being zero in vacuum but it does not contain absorption due to bound states $-\omega_c\,\mathrm{Im}(\varepsilon(\omega_c))\,\langle E^2\rangle-\omega_c\,\mathrm{Im}(\mu(\omega_c))\,\langle H^2\rangle$. The opposite is true for $-\nabla\cdot\boldsymbol{S}$. The net advantage of the latter definition is that when computing the time integrated absorption, corresponding to the well defined energy acquired by matter due to the light pulse,[5] energy transferred to both free and bound charges (the two kinds of constituents considered by the macroscopic approximation of Maxwell equations) is considered. This justifies our earlier choice of definition. The reason why absorption calculated with $-\nabla\cdot\boldsymbol{S}$ is not zero in vacuum is because it also considers local increase and decrease of energy in the electromagnetic field (well-defined in vacuum) as a light pulse propagates, as given by $-\nabla\cdot\boldsymbol{S}=\partial u/\partial t$. We note that, just like in the Abraham-Minkowski controversy, an infinite amount of definitions of absorption exist, and not just the two discussed here [46].

The next simple case we consider, of interest for our metallic sample and transparent substrate at THz frequencies, is the case where one can neglect bound states. In this case, $\boldsymbol{D}=\varepsilon_0\boldsymbol{E}$ and Eq. (6) becomes

$$\frac{\partial}{\partial t}\left(\frac{1}{2}\varepsilon_0\boldsymbol{E}^2+\frac{1}{2}\mu_0\boldsymbol{H}^2\right)+\nabla\cdot(\boldsymbol{E}\times\boldsymbol{H})=-\boldsymbol{J}\cdot\boldsymbol{E}. \qquad (8)$$

The material system is then made of a free electron gas. Integrating this equation over a time window which starts well before the light pulse irradiates the sample and ends well after irradiation (such that overlap between electromagnetic and matter fields can be safely neglected) shows that the time integrated absorption, calculated with any definition, will give the same result, consistently with the fact that bound states are neglected. Equation (8) is then essentially identical to the microscopic Poynting theorem Eq. (1), since $\boldsymbol{B}=\mu_0\boldsymbol{H}$ with the exception that $\boldsymbol{H}$ must be computed with frequency-dependent refractive indices [Eq. (B2)]. This suggests that in this case, the true absorption should be defined as $\boldsymbol{J}\cdot\boldsymbol{E}$. We use the fact that the charge current may in this case be calculated directly from the optical conductivity $\tilde{\sigma}(\omega)$, i.e., $\tilde{n}=\sqrt{1+i\tilde{\sigma}/(\varepsilon_0\omega)}$ [26] to compare both definitions of absorption in Fig. 11, for both optical (a) and THz (b) pulses.

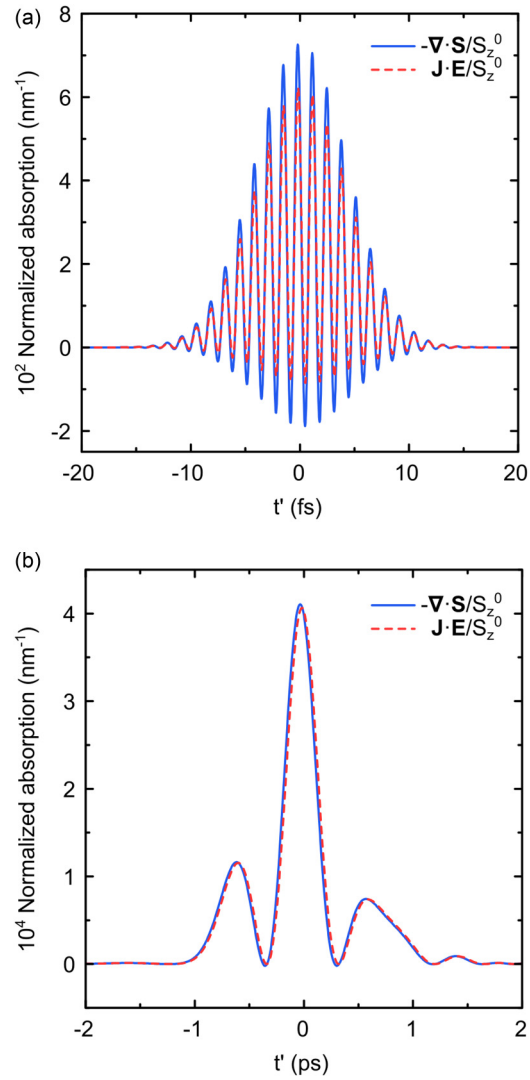

FIG. 11. Comparison of two definitions for (normalized) light absorption, $-\nabla\cdot\boldsymbol{S}/S_z^0$ (blue solid line) and $\boldsymbol{J}\cdot\boldsymbol{E}/S_z^0$ (red dashed line), for both the considered optical (a) and THz (b) light pulses. The time axis has been shifted by defining $t'=t-40$ fs in (a) and $t'=t-10$ ps in (b). The calculation is performed for Pt at the air/Pt interface.

In the optical case, the absorption calculated using $\boldsymbol{J}\cdot\boldsymbol{E}$[6] has the same shape than the absorption calculated using

[5]Long before the light pulse spatially overlaps with the material sample, and long after this irradiation, one can define the energy of the light pulse and matter. The difference of matter energy between two such instants in time is the total energy absorbed.

[6]The charge current is obtained via Ohm's law $\boldsymbol{J}(z,t)=\mathrm{Re}(\sum_n\tilde{\sigma}(\omega_n)(\tilde{\boldsymbol{E}}_n^f(z,t)+\tilde{\boldsymbol{E}}_n^b(z,t)))$, where $\tilde{\boldsymbol{E}}_n^f$ and $\tilde{\boldsymbol{E}}_n^b$ are the complex forward and backward monochromatic (with frequency ω_n) electric field vectors. They are the terms in the sums of Eqs. (B2e) and (B2f) respectively (for s polarization) or Eqs. (B2i) and (B2j) respectively (for p polarization). For instance, at normal incidence

Poynting vector (apart from a small phase shift) but a different amplitude. As explained above, the time integrated absorption will be the same in the absence of bound states. The difference between both definitions will be the amplitude of the nonabsorptive energy transfer (giving rise to negative absorption) which comes from the electromagnetic field induced by the electronic response to the external light pulse [33]. This induced field is more precisely due to electric dipole emission which is taken into account via the optical conductivity.[7] Interestingly, absorption also has a negative part when using $\boldsymbol{J}\cdot\boldsymbol{E}$, because the induced field is included in the total electric field $\boldsymbol{E}$. Equation (8) seems to allow us to exclude the part of the energy transfer purely due the light pulse propagation (the only possible energy transfer in vacuum), in the approximation of no bound state. Nevertheless, in light of Eq. (5) and the corresponding discussion, we cast some doubt about the correctness of the interpretation of $\boldsymbol{J}\cdot\boldsymbol{E}$ as the true time-dependent energy absorption. In addition, it is not clear whether the approximation of no bound state is good in metals at optical frequencies and we still recommend to use $-\boldsymbol{\nabla}\cdot\boldsymbol{S}$ with refractive indices obtained experimentally or from *ab initio* calculations.

The approximation of no bound state is valid when $\widetilde{\sigma}/(\varepsilon_0\omega)$ is sufficiently larger than the permittivity of bound states, that is when the considered frequencies are sufficiently lower than the lowest resonant bound state frequency [24]. This is believed to be true in many metals at THz frequencies [38,39]. However, this condition of low frequency usually implies a large refractive index (both real and imaginary parts) meaning that there will be a large reflection at the air/metal interface. This in turn implies a small electromagnetic field transmission in the sample. According to our previous discussion of Eq. (5), this means that the light and matter fields will be more clearly separated in space, at all times, permitting a separation (to a good approximation) of the electromagnetic and matter energies. This is illustrated in Fig. 11(b) where we computed absorption using both definitions for the THz pulse. The results are almost identical, consistently with the large reflection observed in Fig. 8. The difference between both absorptions is equal to the absorption calculated in Fig. 9(a) in air at the air/Pt interface consistently with Eq. (8) (not shown). This is also consistent with the fact that the calculated absorption in the metallic sample for the THz pulse is mostly positive at all times, meaning that non absorptive effects and then induced fields are negligible.

We finish by noting that, even though a more accurate description of the problem of light-matter interaction necessarily includes coupled equations describing the evolution of the system (as opposed to what was shown for instance in Fig. 6 where absorption calculations are used as an input in equations describing matter), it is possible to describe the energy transfer between light in matter more quantitatively with the formalism shown in this work, in an effective way. One just has to consider time dependence of refractive indices, provided that one has access to temperature (if coupled for instance to the 2TM) or time-dependent refractive indices.

V. CONCLUSION

To conclude, we presented a model to calculate the time-dependent energy transfer from a light pulse to matter when the electromagnetic field and matter is described by macroscopic Maxwell equations and the response of matter is included in refractive indices. Because of the interaction of light with matter, we argued that it is in general not possible to define an absorption because one cannot separate the total energy into energies for light and matter. Still, we argue that if such a quantity needs to be calculated, it is in general better to use $-\boldsymbol{\nabla}\cdot\boldsymbol{S}$ because it includes bound states and is to a good approximation identical to $\boldsymbol{J}\cdot\boldsymbol{E}$ at low frequencies, when the role of bound states is negligible.

We showed that this approach takes chromatic dispersion into account, which becomes important for ultrashort laser pulses, as well as possible phase shifts between different layers and coherent effects which change the temporal shape of the absorption profile. The latter fact is especially important for instance for THz pulses which cannot be modeled as Gaussian pulses in general and whose absorption has been shown to lead to important effects such as ultrafast demagnetization [36]. More effects can easily be taken into account (such as anisotropy or general light polarizations) by using a generalized TMM. Finally, this more general way of computing absorption may find applications for models who need to consider absorptive and nonabsorptive energy transfers on an equal footing.

ACKNOWLEDGMENTS

The authors thank Philippe Scheid, Guillermo Nava Antonio, Maxime Vergés, Julius Hohlfeld, Michel Hehn, Jon Gorchon, Stéphane Mangin, and Grégory Malinowski for valuable discussions. This work is supported by the ANR-20-CE09-0013 UFO, by the Institute Carnot ICEEL for the project CAPMAT and FASTNESS, by the Région Grand Est, by the Metropole Grand Nancy, for the Chaire PLUS by the impact Project LUE-N4S, part of the French PIA project Lorraine Université d'Excellence Reference ANR-15-IDEX-04-LUE, by the FEDERFSE Lorraine et Massif Vosges 2014-2020, a European Union Program, by the European Union's Horizon 2020 research and innovation program COMRAD under the Marie Skłodowska-Curie Grant Agreement No. 861300. This paper is based upon work from COST Action CA17123 MAGNETOFON, supported by COST (European Cooperation in Science and Technology).

and for s polarization, this gives $\boldsymbol{J}(z,t)=\mathrm{Re}(\sum_n \widetilde{\sigma}(\omega_n)(E_n^f(z,t)+E_n^b(z,t))\hat{\boldsymbol{y}})$.

[7]The electric dipole emission in general comes from both free and bound charges as the wave propagation equation $\boldsymbol{\nabla}(\boldsymbol{\nabla}\cdot\boldsymbol{E})-\boldsymbol{\nabla}^2\boldsymbol{E}=-\frac{\partial}{\partial t}(\mu_0\varepsilon_0\frac{\partial \boldsymbol{E}}{\partial t}+\mu_0\boldsymbol{J}+\frac{\partial \boldsymbol{P}}{\partial t})$ shows, where $\boldsymbol{P}$ is the polarization vector. For a complex monochromatic wave of angular frequency ω, the right-hand side of the wave propagation equation becomes $(\omega^2/c^2)\widetilde{\boldsymbol{E}}(\widetilde{\varepsilon}_r+i\widetilde{\sigma}/(\varepsilon_0\omega))=(\omega^2\widetilde{n}^2/c^2)\widetilde{\boldsymbol{E}}$. The linearity (in $\boldsymbol{E}$) of the wave propagation equation justifies our approach. When bound states are negligible, $\boldsymbol{P}=0$ and $\widetilde{\varepsilon}_r=1$.

APPENDIX A: GAUSSIAN OPTICAL LASER PULSE IN VACUUM

In many instances, optical laser pulses can be modeled or treated as having a Gaussian temporal profile. The spectral density is then also given by a Gaussian function:

$$G(\omega) = \frac{\pi c}{\sqrt{2\pi} L \sigma_\omega} e^{-\frac{(\omega-\omega_c)^2}{2\sigma_\omega^2}}. \tag{A1}$$

With σ_ω the standard deviation of the spectral density and ω_c its central angular frequency. Using Eqs. (A1) in (2a) and taking the limit $L \to \infty$:

$$\widetilde{\boldsymbol{E}}(z,t) = E_0 \hat{\boldsymbol{e}} \exp\left(-\frac{\sigma_\omega^2}{2}\left(\frac{z}{c} - t\right)^2 \right) e^{i(k_c z - \omega_c t)} \tag{A2}$$

with $k_c = \omega_c/c$. The electric field is then given by the product of a Gaussian envelop with a monochromatic wave. This does not however justify applying the TMM for the central angular frequency ω_c and subsequently multiplying the absorption by the Gaussian envelop to get the correct propagation and absorption of the laser pulse as this neglects interference between different monochromatic waves as well as chromatic dispersion. The power flow S_z in the direction orthogonal to the sample interface is

$$S_z(z,t) = \frac{E_0^2 \cos(\theta^0)}{\mu_0 c} \cos^2(k_c z - \omega_c t) \times \exp\left(\frac{-1}{2(\sigma_t^I)^2}\left(\frac{z}{c} - t\right)^2 \right). \tag{A3}$$

The standard deviation of the pulse intensity profile $\sigma_t^I = 1/(\sqrt{2}\sigma_\omega)$ is related to the pulse duration $\tau = 2\sqrt{2\ln(2)}\sigma_t^I$ because the latter is the full width at half maximum of the temporal intensity profile by definition. The electric field amplitude on the other hand can be related to the measured laser fluence F [23]:

$$E_0^2 = \frac{2F\mu_0 c}{\sqrt{2\pi}\sigma_t^I\left(1 + e^{-2\left(\sigma_t^I\right)^2 \omega_c^2}\right)}. \tag{A4}$$

As shown by integrating Eq. (A3) over time.

APPENDIX B: EXPRESSIONS FOR ELECTRIC AND MAGNETIC FIELDS IN MATTER

For completeness, we provide here the equations for the electric and magnetic fields inside the heterostructure for both s and p polarizations, which are a generalization of the expressions given in Ref. [20]. We write the incident electric and magnetic fields as follows:

$$\boldsymbol{k}^i = \frac{2\pi}{\lambda_n}(\cos(\theta^0)\hat{\boldsymbol{z}} + \sin(\theta^0)\hat{\boldsymbol{x}}), \tag{B1a}$$

$$E_n^i(\boldsymbol{r},t) = E_0 G(\omega_n) e^{i(\boldsymbol{k}^i\cdot\boldsymbol{r} - \omega_n t)}, \tag{B1b}$$

$$(\mathrm{s}): \quad \boldsymbol{E}^i(\boldsymbol{r},t) = \hat{\boldsymbol{y}}\,\mathrm{Re}\left[\sum_n E_n^i(\boldsymbol{r},t)\right], \tag{B1c}$$

$$\boldsymbol{H}^i(\boldsymbol{r},t) = \frac{1}{c\mu_0}(\sin(\theta^0)\hat{\boldsymbol{z}} - \cos(\theta^0)\hat{\boldsymbol{x}}) \times \mathrm{Re}\left[\sum_n E_n^i(\boldsymbol{r},t)\right], \tag{B1d}$$

$$(\mathrm{p}): \quad \boldsymbol{E}^i(\boldsymbol{r},t) = (-\sin(\theta^0)\hat{\boldsymbol{z}} + \cos(\theta^0)\hat{\boldsymbol{x}}) \times \mathrm{Re}\left[\sum_n E_n^i(\boldsymbol{r},t)\right], \tag{B1e}$$

$$\boldsymbol{H}^i(\boldsymbol{r},t) = \frac{1}{c\mu_0}\hat{\boldsymbol{y}}\,\mathrm{Re}\left[\sum_n E_n^i(\boldsymbol{r},t)\right]. \tag{B1f}$$

Where we have kept the spatial dependence in $\boldsymbol{r} = (x,y,z)$ for generality, $\lambda_n = 2\pi c/\omega_n$ is the wavelength of the monochromatic wave n in vacuum and the geometry is defined by Fig. 1.

In the heterostructure, the various electric field amplitudes E_{0n}^f and E_{0n}^b of the respective forward and backward monochromatic plane wave modes, as well as the wave vector (complex) angles θ_n with respect to the air/sample surface normal, are directly obtained from the TMM code of Byrnes[8] [20]. The total fields in the heterostructure (separating forward and backward propagation) are

$$\boldsymbol{k}_n^f = \frac{2\pi\widetilde{n}_n}{\lambda_n}(\cos(\theta_n)\hat{\boldsymbol{z}} + \sin(\theta_n)\hat{\boldsymbol{x}}), \tag{B2a}$$

$$\boldsymbol{k}_n^b = \frac{2\pi\widetilde{n}_n}{\lambda_n}(-\cos(\theta_n)\hat{\boldsymbol{z}} + \sin(\theta_n)\hat{\boldsymbol{x}}), \tag{B2b}$$

$$E_n^f(\boldsymbol{r},t) = E_{0n}^f G(\omega_n) e^{i(\boldsymbol{k}_n^f\cdot\boldsymbol{r} - \omega_n t)}, \tag{B2c}$$

$$E_n^b(\boldsymbol{r},t) = E_{0n}^b G(\omega_n) e^{i(\boldsymbol{k}_n^b\cdot\boldsymbol{r} - \omega_n t)}, \tag{B2d}$$

$$(\mathrm{s}): \quad \boldsymbol{E}^f(\boldsymbol{r},t) = \hat{\boldsymbol{y}}\,\mathrm{Re}\left[\sum_n E_n^f(\boldsymbol{r},t)\right], \tag{B2e}$$

$$\boldsymbol{E}^b(\boldsymbol{r},t) = \hat{\boldsymbol{y}}\,\mathrm{Re}\left[\sum_n E_n^b(\boldsymbol{r},t)\right], \tag{B2f}$$

$$\boldsymbol{H}^f(\boldsymbol{r},t) = \mathrm{Re}\left[\sum_n \frac{\widetilde{n}_n}{c\mu_0}(\sin(\theta_n)\hat{\boldsymbol{z}} - \cos(\theta_n)\hat{\boldsymbol{x}})E_n^f(\boldsymbol{r},t)\right], \tag{B2g}$$

$$\boldsymbol{H}^b(\boldsymbol{r},t) = \mathrm{Re}\left[\sum_n \frac{\widetilde{n}_n}{c\mu_0}(\sin(\theta_n)\hat{\boldsymbol{z}} + \cos(\theta_n)\hat{\boldsymbol{x}})E_n^b(\boldsymbol{r},t)\right], \tag{B2h}$$

$$(\mathrm{p}): \quad \boldsymbol{E}^f(\boldsymbol{r},t) = \mathrm{Re}\left[\sum_n (-\sin(\theta_n)\hat{\boldsymbol{z}} + \cos(\theta_n)\hat{\boldsymbol{x}})E_n^f(\boldsymbol{r},t)\right], \tag{B2i}$$

[8] In the code of Ref. [20], the amplitudes are given for $E_0 = 1$.

$$\boldsymbol{E}^b(\boldsymbol{r},t) = \mathrm{Re}\left[\sum_n(-\sin(\theta_n)\hat{\boldsymbol{z}} - \cos(\theta_n)\hat{\boldsymbol{x}})E_n^b(\boldsymbol{r},t)\right], \quad \text{(B2j)}$$

$$\boldsymbol{H}^f(\boldsymbol{r},t) = \mathrm{Re}\left[\sum_n \frac{\widetilde{n}_n}{c\mu_0}\hat{\boldsymbol{y}}E_n^f(\boldsymbol{r},t)\right], \quad \text{(B2k)}$$

$$\boldsymbol{H}^b(\boldsymbol{r},t) = \mathrm{Re}\left[\sum_n \frac{\widetilde{n}_n}{c\mu_0}\hat{\boldsymbol{y}}E_n^b(\boldsymbol{r},t)\right]. \quad \text{(B2l)}$$

The total fields are then given by $\boldsymbol{E} = \boldsymbol{E}^f + \boldsymbol{E}^b$ and $\boldsymbol{H} = \boldsymbol{H}^f + \boldsymbol{H}^b$.

APPENDIX C: THZ PULSE SPECTRAL DENSITY

The spectral density for the THz pulse considered in this work is given by

$$G(\omega) = F(\omega,\lambda_0,\tau) + e^{i\alpha(\omega-\omega_c)}F(\omega,\lambda_0',\tau') \quad \text{(C1)}$$

with $\omega_c = 2\pi c/\lambda_0$ and the function F defined by

$$F(\omega,\lambda,\tau) = \frac{\pi c}{L}\frac{s\exp\left(\left(s\frac{2\pi c}{\lambda}\right)\ln(\omega\tau)\right)e^{-\omega\tau}}{\Gamma\left(s\frac{2\pi c}{\lambda}+1\right)}, \quad \text{(C2)}$$

where Γ is the gamma function and we have used $\lambda_0 = 0.33$ mm, $\lambda_0' = 0.05\lambda_0$, $\tau = 1$ps, $\tau' = 10\tau$, $\alpha = 1.4$ ps, and $s = 10^{-12}$ is a scaling factor used to avoid large numbers when numerically computing the spectral density.

[1] G. L. Eesley, Phys. Rev. Lett. **51**, 2140 (1983).
[2] W. S. Fann, R. Storz, H. W. K. Tom, and J. Bokor, Phys. Rev. Lett. **68**, 2834 (1992).
[3] S. K. Sundaram and E. Mazur, Nat. Mater. **1**, 217 (2002).
[4] E. Beaurepaire, J.-C. Merle, A. Daunois, and J.-Y. Bigot, Phys. Rev. Lett. **76**, 4250 (1996).
[5] A. Stupakiewicz, K. Szerenos, D. Afanasiev, A. Kirilyuk, and A. V. Kimel, Nature (London) **542**, 71 (2017).
[6] J. Wang, C. Sun, J. Kono, A. Oiwa, H. Munekata, Ł. Cywiński, and L. J. Sham, Phys. Rev. Lett. **95**, 167401 (2005).
[7] C. Guillemard, W. Zhang, G. Malinowski, C. de Melo, J. Gorchon, S. Petit-Watelot, J. Ghanbaja, S. Mangin, P. Le Fèvre, F. Bertran, and S. Andrieu, Adv. Mater. **32**, 1908357 (2020).
[8] M. Beck, M. Klammer, S. Lang, P. Leiderer, V. V. Kabanov, G. N. Gol'tsman, and J. Demsar, Phys. Rev. Lett. **107**, 177007 (2011).
[9] F. Blanchard, L. Razzari, H.-C. Bandulet, G. Sharma, R. Morandotti, J. C. Kieffer, T. Ozaki, M. Reid, H. F. Tiedje, H. K. Haugen, and F. A. Hegmann, Opt. Express **15**, 13212 (2007).
[10] J. Krüger and W. Kautek, *Polymers and Light*, edited by T. K. Lippert (Springer, Berlin, Heidelberg, 2004), pp. 247–290.
[11] E. Runge and E. K. U. Gross, Phys. Rev. Lett. **52**, 997 (1984).
[12] F. Töpler, J. Henk, and I. Mertig, New J. Phys. **23**, 033042 (2021).
[13] M. I. Kaganov, I. M. Lifshitz, and L. V. Tanatarov, ZhETF **31**, 232 (1957) [Sov. Phys. JETP **4**, 173 (1957)].
[14] D. M. Nenno, R. Binder, and H. C. Schneider, Phys. Rev. Appl. **11**, 054083 (2019).
[15] J. Zak, E. R. Moog, C. Liu, and S. D. Bader, Phys. Rev. B **43**, 6423 (1991).
[16] M. Schubert, Phys. Rev. B **53**, 4265 (1996).
[17] D. L. Windt, Comput. Phys. **12**, 360 (1998).
[18] J. S. C. Prentice, J. Phys. D **33**, 3139 (2000).
[19] C. C. Katsidis and D. I. Siapkas, Appl. Opt. **41**, 3978 (2002).
[20] S. J. Byrnes, arXiv:1603.02720.
[21] N. C. Passler and A. Paarmann, J. Opt. Soc. Am. B **34**, 2128 (2017).
[22] S. Bonetti, M. C. Hoffmann, M.-J. Sher, Z. Chen, S.-H. Yang, M. G. Samant, S. S. P. Parkin, and H. A. Dürr, Phys. Rev. Lett. **117**, 087205 (2016).
[23] Q. Remy, Ph.D. thesis, Université de Lorraine, 2021.
[24] J. D. Jackson, *Classical Electrodynamics*, 3rd ed. (John Wiley & Sons, New York, 1999).
[25] Y. Yang, S. Dal Forno, and M. Battiato, Phys. Rev. B **104**, 155437 (2021).
[26] In certain instances, refractive indices may be determined from the relative permittivity of bound states $\widetilde{\varepsilon}_r$ and complex conductivities $\widetilde{\sigma}$ via $\widetilde{n} = \sqrt{\widetilde{\varepsilon}_r + i\widetilde{\sigma}/(\varepsilon_0\omega)}$. For metals at THz frequencies, one usually has $\widetilde{\varepsilon}_r = 1$.
[27] M. N. Polyanskiy, Refractive Index database, https://refractiveindex.info.
[28] W. S. M. Werner, K. Glantschnig, and C. Ambrosch-Draxl, J. Phys. Chem. Ref. Data **38**, 1013 (2009).
[29] K. M. McPeak, S. V. Jayanti, S. J. P. Kress, S. Meyer, S. Iotti, A. Rossinelli, and D. J. Norris, ACS Photonics **2**, 326 (2015).
[30] M. Obergfell and J. Demsar, Phys. Rev. Lett. **124**, 037401 (2020).
[31] J. Igarashi, Q. Remy, S. Iihama, G. Malinowski, M. Hehn, J. Gorchon, J. Hohlfeld, S. Fukami, H. Ohno, and S. Mangin, Nano Lett. **20**, 8654 (2020).
[32] C. Pellegrini, S. Sharma, J. K. Dewhurst, and A. Sanna, Phys. Rev. B **105**, 134425 (2022).
[33] P. Scheid, Q. Remy, S. Lebégue, G. Malinowski, and S. Mangin, J. Magn. Magn. Mater. **560**, 169596 (2022).
[34] J. Kimling and D. G. Cahill, Phys. Rev. B **95**, 014402 (2017).
[35] J. Neu and C. A. Schmuttenmaer, J. Appl. Phys. **124**, 231101 (2018).
[36] M. Shalaby, A. Donges, K. Carva, R. Allenspach, P. M. Oppeneer, U. Nowak, and C. P. Hauri, Phys. Rev. B **98**, 014405 (2018).
[37] A. L. Chekhov, Y. Behovits, J. J. F. Heitz, C. Denker, D. A. Reiss, M. Wolf, M. Weinelt, P. W. Brouwer, M. Münzenberg, and T. Kampfrath, Phys. Rev. X **11**, 041055 (2021).
[38] T. S. Seifert, N. M. Tran, O. Gueckstock, S. M. Rouzegar, L. Nadvornik, S. Jaiswal, G. Jakob, V. V. Temnov, M. Münzenberg, M. Wolf, M. Kläui, and T. Kampfrath, J. Phys. D **51**, 364003 (2018).
[39] Z. Wang, Y. Han, N. Xu, L. Chen, C. Li, L. Wu, and W. Zhang, IEEE Trans. Terahertz Sci. Technol. **8**, 161 (2018).
[40] Y. Zhao and D. R. Grischkowsky, IEEE Trans. Microwave Theory Tech. **55**, 656 (2007).

[41] F. Richter, M. Florian, and K. Henneberger, EPL (Europhysics Letters) **81**, 67005 (2008).
[42] M. G. Silveirinha, Phys. Rev. B **80**, 235120 (2009).
[43] M. G. Silveirinha, Phys. Rev. B **82**, 037104 (2010).
[44] W. Heitler, *The Quantum Theory of Radiation*, 3rd ed., edited by N. F. Mott and E. C. Bullard (Clarendon Press, Oxford, 1954).
[45] I. Campos and J. L. Jimenez, European J. Phys. **13**, 117 (1992).
[46] R. N. C. Pfeifer, T. A. Nieminen, N. R. Heckenberg, and H. Rubinsztein-Dunlop, Rev. Mod. Phys. **79**, 1197 (2007).
[47] G. D. Mahan, *Many-Particle Physics*, 3rd ed. (Springer Science & Business Media, New York, 2000).
[48] F. Richter, K. Henneberger, and M. Florian, Phys. Rev. B **82**, 037103 (2010).